



Article

Pressure-Assisted Lubrication of DC01 Steel Sheets to Reduce Friction in Sheet-Metal-Forming Processes

Tomasz Trzepieciński ^{1,*}, Krzysztof Sz wajka ² and Marek Szewczyk ²

¹ Department of Manufacturing Processes and Production Engineering, Rzeszow University of Technology, al. Powst. Warszawy 8, 35-959 Rzeszów, Poland

² Department of Integrated Design and Tribology Systems, Faculty of Mechanics and Technology, Rzeszow University of Technology, ul. Kwiatkowskiego 4, 37-450 Stalowa Wola, Poland

* Correspondence: tomtrz@prz.edu.pl

Abstract: Friction in sheet-metal-forming processes not only affects the values of the force parameters of the process but also determines the quality of the surface of the drawpieces. This paper presents an approach to reducing the coefficient of friction by directly applying pressurized oil to the contact zone. For this purpose, a special test stand was built to carry out the strip draw test, commonly used to model the phenomenon of friction in the deep-drawing process. This test consisted of pulling a strip between flat countersamples made of 145Cr6 cold-work tool steel covered with an abrasion-resistant Mtec (AlTiN) coating. During the pilot tests, various contact pressures, lubricants with different viscosities, and different lubricant pressures were used. The influence of friction conditions on the surface roughness of the samples and the relationship between the friction conditions and the value of the coefficient of friction were determined. The supply of the lubricant under pressure into the contact zone has a beneficial effect on reducing friction. The coefficient of friction decreases with increasing lubricant pressure for contact pressures of 2–6 MPa. For a contact pressure of 8 MPa, the lubricant pressure is the least favorable for reducing the coefficient of friction. At higher lubricant pressures (12 and 18 bar), the lubrication efficiency depends on the viscosity of the lubricant and decreases with increasing contact pressure.

Keywords: deep drawing; lubrication; metal forming; coefficient of friction



Citation: Trzepieciński, T.; Sz wajka, K.; Szewczyk, M. Pressure-Assisted Lubrication of DC01 Steel Sheets to Reduce Friction in Sheet-Metal-Forming Processes. *Lubricants* **2023**, *11*, 169. <https://doi.org/10.3390/lubricants11040169>

Received: 23 March 2023

Revised: 3 April 2023

Accepted: 7 April 2023

Published: 8 April 2023



Copyright: © 2023 by the authors. Licensee MDPI, Basel, Switzerland. This article is an open access article distributed under the terms and conditions of the Creative Commons Attribution (CC BY) license (<https://creativecommons.org/licenses/by/4.0/>).

1. Introduction

Sheet metal forming (SMF) is the basic method for processing sheet metal and thin-walled load-bearing components in the automotive industry [1]. To ensure the appropriate surface of the products, it is necessary to provide appropriate friction conditions, and the lower the friction, the better the surface finish of deep-drawn components [2]. Knowledge of the mechanisms that occur in friction and lubrication processes also allows for the construction of tools that wear to a minimum extent during operation and are characterized by reliability and durability [3]. The work efficiency of stamping tools and the surface quality of products primarily depend on the operational properties of the surface layer of the tool, in particular, its resistance to thermal, tribological, and fatigue wear [4,5]. Knowledge of the mechanisms of friction and wear is the foundation for understanding the problem of selecting the right material and forming the technology for the production of a specific component [6].

During the plastic forming of metallic sheets, the summits of the asperities, under the influence of pressure forces, are plastically deformed until the resulting contact surface is sufficient to transfer the load [7]. Shearing and elastic–plastic deformation of the surface asperities occur during sheet metal forming, which increases the real contact area [8]. The sliding velocity [9,10], contact pressure [11], surface texture [12,13], tool roughness [2], as well as lubrication conditions [14,15] affect the change of surface roughness of sheet metal in the deep-drawing process. Therefore, surface roughness is not constant during SMF.

During the SMF processes, there are zones of material that differ in terms of sliding velocity, contact pressures, and lubrication conditions. The strip drawing test (SDT) consists of drawing the strip specimen clamped between countersamples with a rounded [16,17] or flat working surface [18].

The most effective way to reduce the impact of friction on the course of the SMF operations is lubrication [19]. The most important properties of the lubricant from the point of view of its use in plastic-forming processes are the viscosity and boundary lubrication effect [20]. During the deformation process, the lubricant reduces the contact pressures and coefficient of friction (COF) [21,22]. In the literature, there are many studies on the efficiency of lubricants of various origins (refined, petroleum-derived, synthetic, natural) and of various consistencies (solid, liquid, emulsions) and viscosities [23,24].

The combination of modern coatings (nanostructured, nanolayered, nanocomposite, etc.) with the design of self-lubricating tools containing microchannels and pockets constituting a reservoir of lubricants is a very promising and effective way to increase the efficiency of lubrication under high-pressure conditions [25]. Among the many shapes of texturing depressions, for example, crossed and parallel channels [26], triangular depressions [27], square depressions [28], and more complex shapes [29], the most frequently studied structures are spherical depressions [30] due to the ease of fabrication [31]. In addition, the density of the pits plays an important role as it affects the relubrication process of the sheet metal surface as it travels over the tool surface. Textures can have a preferential direction or be randomly arranged [32]. The lubricant viscosity, thickness of the lubricating film, and sliding velocity affect the optimum distance between the depressions [33,34]. Metal sheets produced by the cold-rolling process exhibit a surface topography that consists of valleys that naturally act as a lubricant reservoir [35,36].

Lubrication is essential to ensure the efficiency of the SMF processes in terms of component surface quality and acceptable sheet deformations. The selection of the type of the lubricant is crucial to achieving reducing friction. The valleys in the surface topography that contain the lubricating oil under high-pressure conditions form a kind of lubrication cushion. Under the influence of contact pressure, the pressure of the lubricant in the pockets increases, but, at the same time, the share of the mechanical cooperation of the rubbing surfaces increases. Many researchers focus on the study of the impact of oil viscosity and the type of the lubricant on the reduction of the coefficient of friction. Meanwhile, works aimed at increasing the lubricant pressure on the contact surface, and thus the lubrication efficiency, are limited in the literature.

In order to provide better surface separation in conditions where the surface topography does not contain closed oil pockets of sufficient volume, this article proposes a new approach to lubricating the sheet surface with pressurized oil directly delivered to the contact zone in the blankholder area in SMF. Studies were carried out using the SDT, the most frequently used tribotest to analyze friction conditions in SMF [37,38]. Strip drawing tests were carried out using a specially designed tester equipped with an Argo-Hytos hydraulic power pack. Cold-rolled low-carbon DC01 steel sheets commonly used in the automotive industry were used as the test material. Different contact pressures and different pressure values of oil with different viscosities were tested. The influence of friction conditions on the surface roughness parameters (S_q , S_{sk} , S_{ku} , S_z) of the samples and the relationship between the friction conditions and the value of the coefficient of friction were determined.

2. Material and Methods

2.1. Test Material

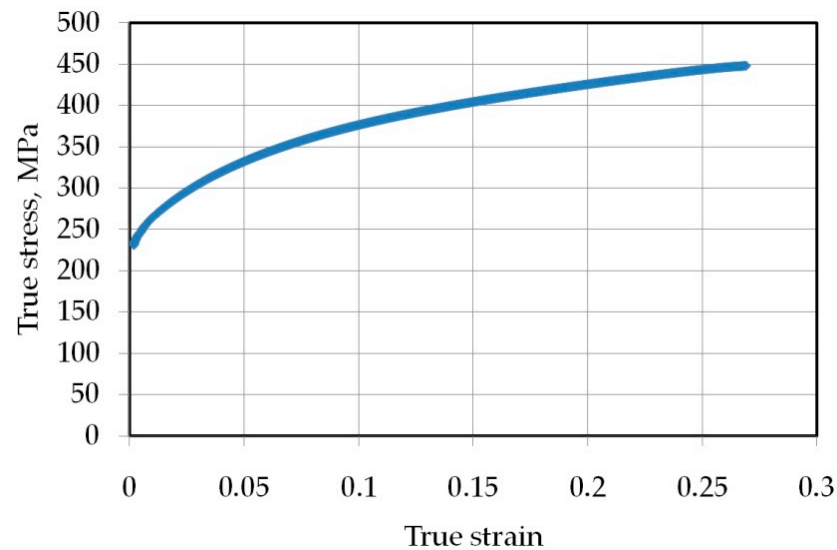
A cold-rolled low-carbon DC01 steel sheet was used as the test material. This steel, due to its high ductility, is very often used in the automotive industry. Quality requirements for the chemical composition and basic mechanical properties (yield stress $R_{p0.2}$, ultimate tensile stress R_m , and elongation A_t) of the DC01 steel determined in the uniaxial tensile test are presented in Tables 1 and 2, respectively. True stress–true strain curves for three specimens cut along the sheet-rolling direction are shown in Figure 1.

Table 1. Chemical composition (max. wt.%) of DC01 steel sheet according to EN 10130:2006 standard.

Carbon	Manganese	Phosphorus	Sulfur	Iron
0.12	0.6	0.045	0.045	Balance

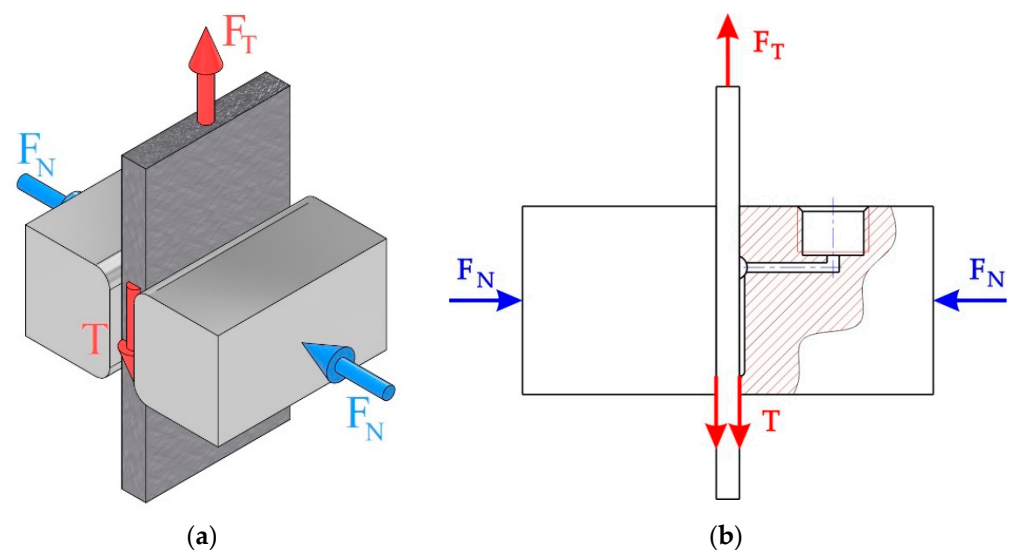
Table 2. Basic mechanical parameters of DC01 steel sheet.

$R_{p0.2}$, MPa	R_m , MPa	A_t , %	Hardness HV
231.5	348.1	38.5	105

**Figure 1.** True stress–strain curve of DC01 steel sheet.

2.2. Friction Test

The values of the COF of the DC01 steel sheet were determined using the SDT (Figure 2a). This test consisted of pulling a strip specimen between two countersamples made of 145Cr6 cold-work steel, whose working surface was additionally covered with an abrasion-resistant Mtec (AlTiN) coating. The pressurized lubricant was directly supplied to the contact zone using special channels drilled in both countersamples (Figure 2b).

**Figure 2.** (a) Schematic of strip drawing test and (b) cross-section of countersamples: F_N —contact force, F_T —pulling force, and T —friction force.

Strip drawing tests were carried out using a specially designed tester (Figure 3c), mounted in the Z100 (Zwick/Roell) uniaxial tensile testing machine. Samples in the form of a sheet metal strip with dimensions of 130 mm (length) \times 25 mm (width) \times 1 mm (thickness) were pulled between the countersamples with adjustable contact pressure. The friction force was recorded using the measuring system testing machine, while the normal force was recorded using Labview program based on the indications of the force sensor type 9345B (Kistler, Winterthur, Switzerland). The values of these two forces were correlated in Labview program using a Megatron Series SPR18 displacement sensor (Figure 3a). In addition, in order to carry out SDTs with the use of pressure-assisted lubrication, the stand was equipped with an Argo-Hytos hydraulic power pack (Baar, Switzerland) (Figure 3b), with the parameters presented in Table 3.

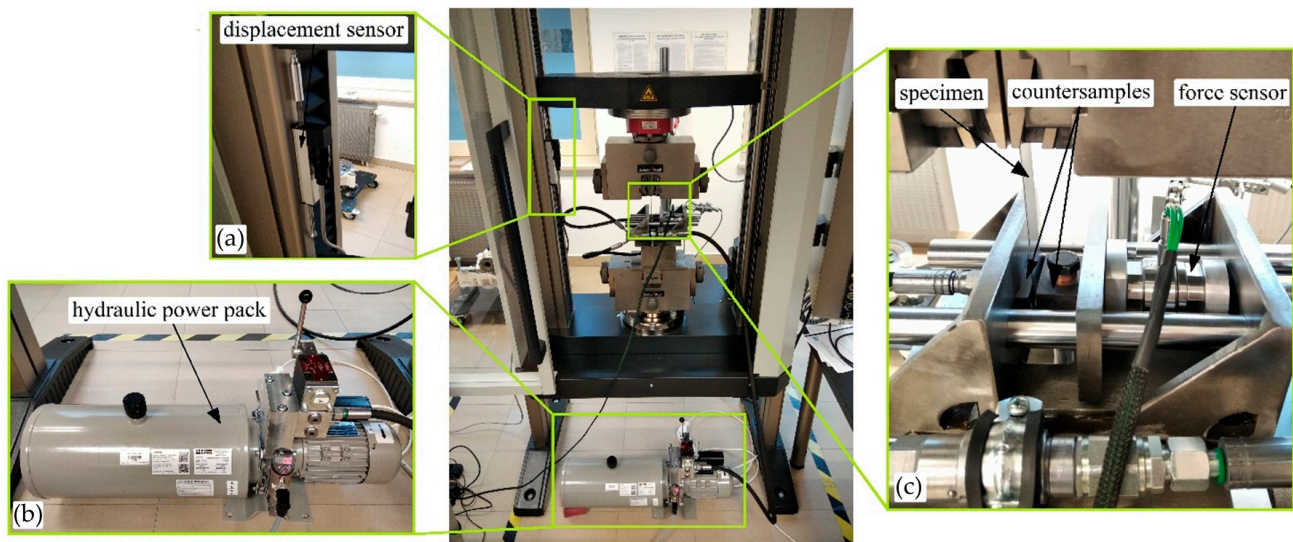


Figure 3. Test stand: (a) displacement sensor, (b) hydraulic feeder, and (c) friction tester.

Table 3. Basic parameters of hydraulic feeder.

Parameter	Value	Unit
Flow	0.4	L/min
Maximum pressure	63	bar
Power	0.18	kW
Working temperature	−25 ... +50	°C

Based on the values of the normal force F_N and corresponding pulling (friction) force F_T , the values of the COF μ were determined by Equation (1).

$$\mu = \frac{F_T}{2 \cdot F_N} \quad (1)$$

The tests were carried out using oils typically applied for metal-forming operations. The kinematic viscosity of the oils used is presented in Table 4. The tests were carried out at nominal contact pressures p_N of 2, 4, 6, and 8 MPa and variable lubrication pressures p_L of 0, 6, 12, and 18 bars, respectively. The nominal contact pressure was determined as a ratio of the contact force and contact area of the sheet with the countersamples. In the deep-drawing process, the blankholding pressure applied in the flange region during drawing varies in the range of 1 MPa to 4 MPa depending on the strength of the blank material [39,40]. It should be emphasized that nominal contact pressure conditions do not represent real tribological conditions in SMF. The real contact pressure is greater than the nominal pressure and is not constant over the entire contact area of the surface asperities of the tool and workpiece. The

surface of cold-rolled sheets is characterized by a random distribution of surface asperities and valleys. Moreover, the real contact area is constantly evolving.

Table 4. Basic physical parameters of oils tested.

Oil	Kinematic Viscosity at 40 °C, mm ² /s
S100 Plus oil for deep-drawing (Naftochem)	110
S300 oil for deep-drawing operations (Naftochem)	300

2.3. Surface Topography

The basic height parameters of the geometric structure and surface topography (5 × 5 mm) (Figure 4b) were determined using a T8000RC stationary profilometer (Figure 4a) from Jenoptik AG (Jena, Germany) in accordance with the ISO 25178-2 [41] standard. In order to compare changes in the surface roughness due to friction, measurements of the surface roughness were carried out before and after the friction tests. The surface topography of the DC01 steel sheet is shown in Figure 4b. The basic roughness parameters of the DC01 steel sheet and countersamples are shown in Table 5. The topography of the surfaces of the strip specimens was examined using a MIRA3 scanning electron microscope (SEM) (Tescan, Brno, Czech Republic). The SEM micrograph of the surface of the as-received DC01 steel sheet is shown in Figure 5. The hardnesses of countersamples material and AlTiN coating as an average from six measurements are 250.7 HV 10 and 2714 HV 0.05, respectively.

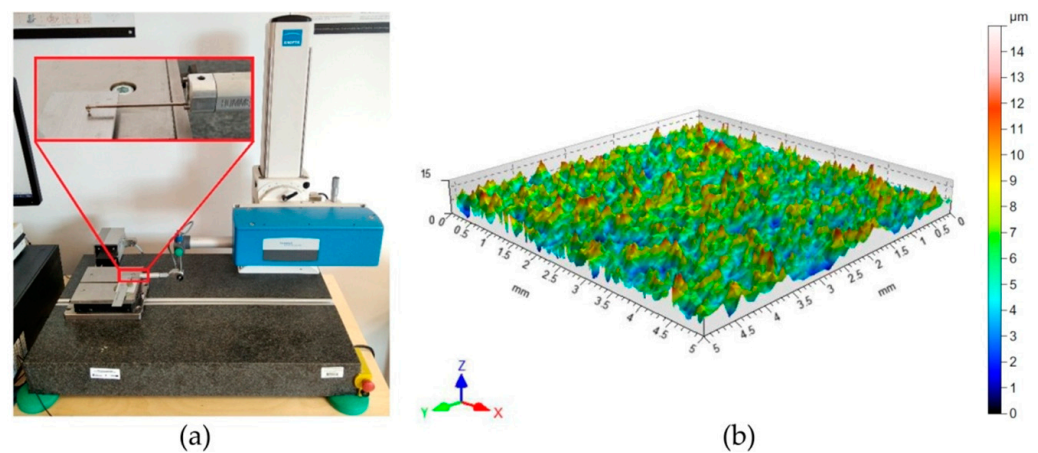


Figure 4. (a) Hommel—Etamic T8000RC profilometer and (b) topography of DC01 steel sheet in as-received state.

Table 5. Basic surface roughness parameters of test material.

Surface Roughness Parameter	Value	
	Sheet Metal	Countersamples
Root mean square roughness Sq, μm	1.82	0.384
Surface skewness Ssk	0.553	−2.87
Surface kurtosis Sku	3.32	24.7
Highest peak of the surface Sp, μm	9.13	4.28
Maximum pit depth Sv, μm	5.31	6.50
10-point peak-valley surface roughness Sz, μm	14.4	10.8
Average roughness Sa, μm	1.44	0.237

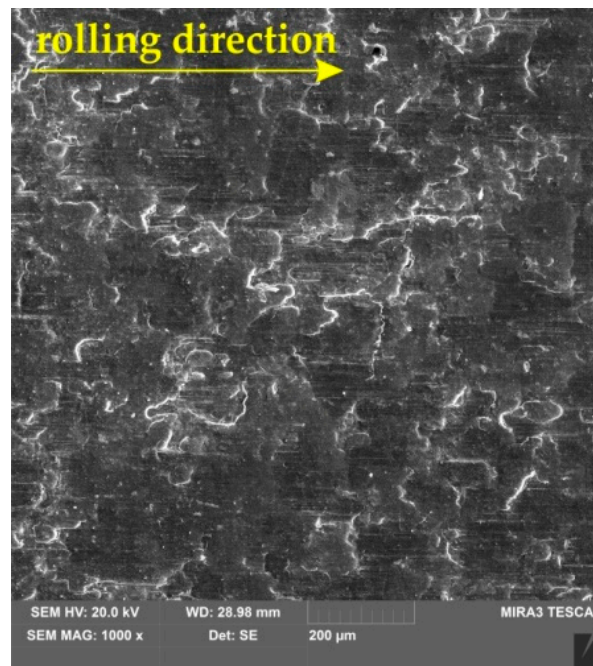


Figure 5. SEM micrograph of the surface of DC01 sheet metal.

3. Results and Discussion

3.1. Coefficient of Friction

The value of the COF decreases as the lubricant pressure increases for contact pressures of $p_N = 2\text{--}6$ MPa (Figure 6). For a contact pressure of 8 MPa, the lubricant pressure exerts the least favorable effect of reducing the COF. Only after exceeding the contact pressure of 6 bar does the lubricant pressure clearly reduce the COF value. With an increase in pressure, the pressure of the lubricant in the closed oil pockets increases, but, at the same time, the share of the mechanical interaction of the surface asperities in the total friction resistance increases. Increasing oil pressure has a positive effect on reducing friction, but its value is limited by the possible occurrence of leaks from the contact zone. It should be emphasized that, in the range of the parameters of the friction test, such leaks were not observed.

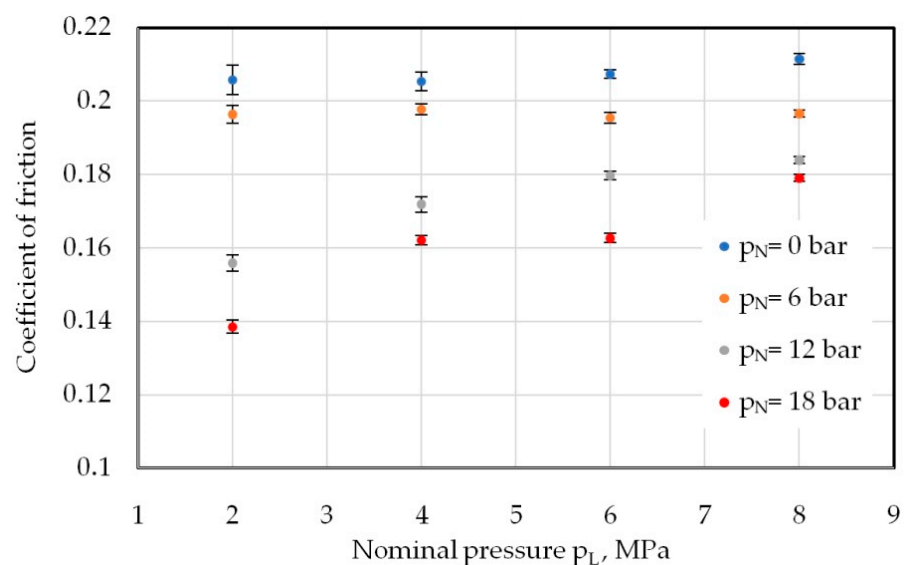


Figure 6. Effect of nominal pressure on the COF of specimens lubricated with S100 Plus oil.

In the range of contact pressures of $p_N = 2\text{--}8$ MPa, which occur in the blankholder area in SMF [39,40,42], the value of the COF shows the tendency to increase with increasing contact pressure (Figure 6). According to Cillauren et al. [42], Djordjević et al. [43], Evin et al. [16], Filzek and Groche [44], and Bay et al. [37] (Figure 7), friction conditions in the blankholder area in SMF are determined using a strip drawing test with flat dies. Moreover, the researchers of the Friedrich-Alexander-Universität Erlangen-Nürnberg [45] concluded that a strip drawing test with flat dies “models the tribological conditions of the area between blank holder and die in a conventional deep drawing process”. A strip drawing test with flat dies is also commonly used to examine the tribological effects of lubricants in SMF [46] and the effect of the surface texture of the sheet in the final tribological conditions at the interface [47].

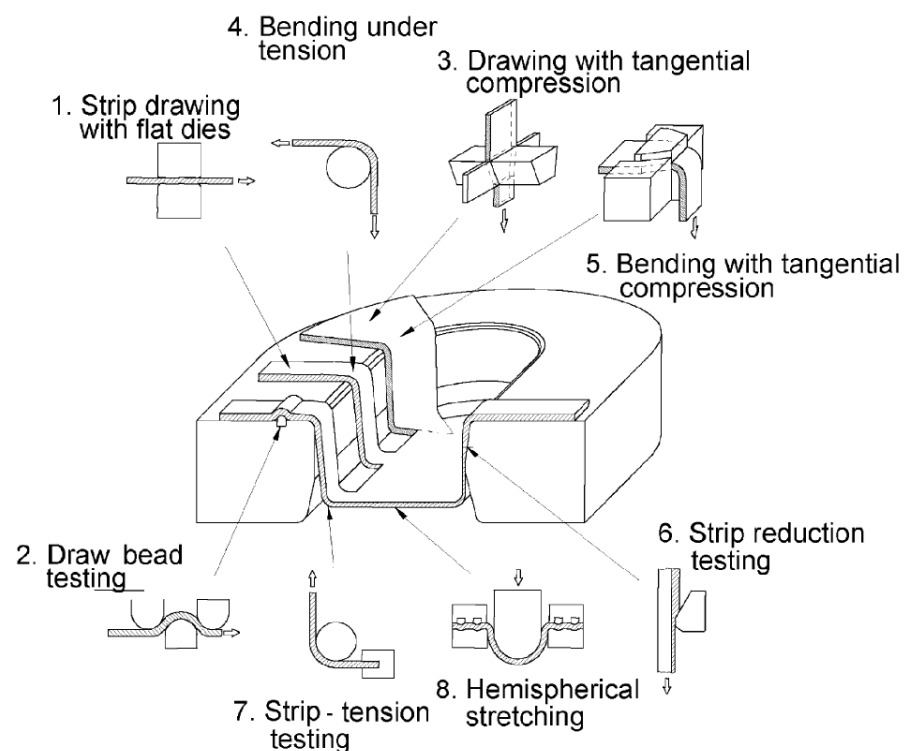


Figure 7. Simulative tests for sheet metal forming (Reprinted with permission from Ref. [37]; copyright © 2007 Elsevier Ltd. All rights reserved).

Conventional lubrication ($p_L = 0$ MPa) with S100 Plus oil, without the forced supply of the pressurized lubricant, causes only a slight increase in the COF. However, under the conditions of lubrication with the pressurized lubricant, the decrease in the COF is evident. For a contact pressure of 2 MPa, the lubricant under 18 bar of pressure reduced the value of the COF by about 33% compared with lubrication without forced lubricant pressure. It should be emphasized that during traditional lubrication without forced lubricant pressure, the contact pressure causes an increase in the lubricant pressure in closed lubricant pockets [48,49]. However, as research has shown, this effect can be multiplied by supplying the lubricant under pressure to the contact zone.

When lubricated with S100 Plus oil (Figure 6), there is a tendency to stabilize the COF with increasing lubricant pressure. A different relationship occurs during friction tests with S300 oil, which is three times more viscous. The direction of the inflection of the curves shows that the lubrication efficiency has a tendency to increase with increasing lubricant pressure (Figure 8). The higher viscosity of the lubricant allows the development of the interaction of the surface asperities to be delayed.

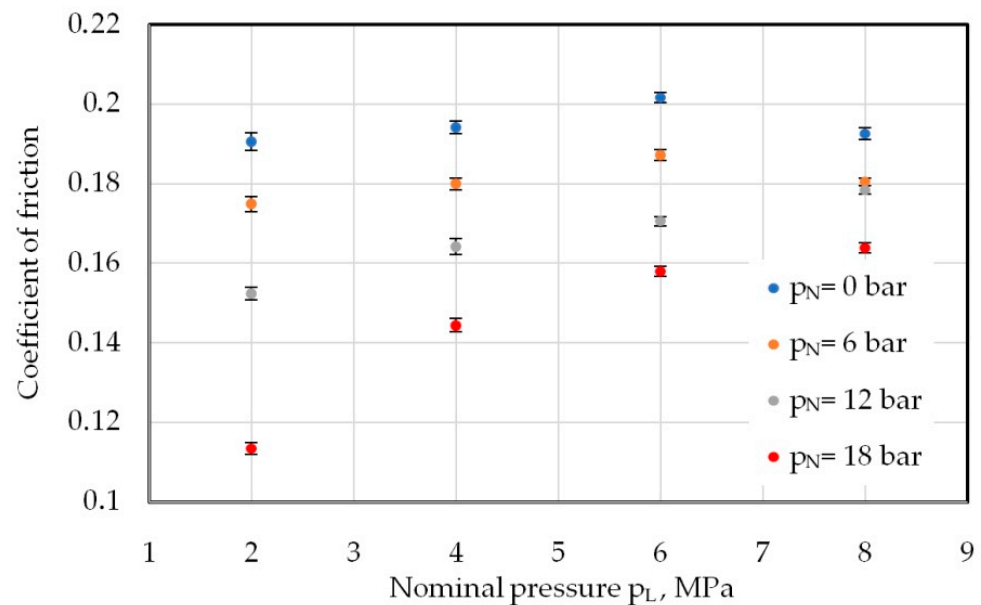


Figure 8. Effect of nominal pressure on COF for lubrication with S300 oil.

As expected, the lubricant at the highest forced pressure ($p_L = 18$ bar) reduced the COF value the most (Figure 8). At a contact pressure of $p_N = 2$ MPa, the COF decreased by about 39%, and at $p_N = 8$ MPa, it decreased by about 15% compared with lubrication without forced pressure ($p_L = 0$ bar). Therefore, in order to ensure optimal lubrication conditions and reduce friction, pressure-assisted lubrication should be applied with oil of an appropriate viscosity adjusted to the value of the contact pressures occurring in the contact zone.

For the tests carried out at $p_L = 0$ bar and $p_L = 6$ bar, the COF remains quite constant. With the increase in the oil pressure to $p_L = 12$ bar, the value of the COF increased in the range of the analyzed contact pressures, with a visible tendency to stabilization after exceeding the pressure of $p_N = 8$ MPa. In the range of small contact pressures p_N , applying pressurized oil is most effective in reducing the COF. Increasing the contact pressure p_N reduces the beneficial effect of the oil pressure p_L by the intensification of the mechanical interaction of the surface asperities.

3.2. Effectiveness of Lubrication

The effectiveness of lubrication κ_L was determined in relation to the coefficient of friction μ_0 obtained under the lubricant pressure of $p_L = 0$ bar:

$$\kappa_L = \frac{\mu_0 - \mu_p}{\mu_0} \times 100\% \quad (2)$$

where μ_p is the COF obtained at a lubricant pressure of $p_L > 0$ bar.

The lubrication efficiency of S100 Plus oil when tested under pressure $p_L = 6$ bar slightly increases (from about 4.8% to about 7%) with increasing contact pressure (Figure 9). At higher lubricant pressures, the lubrication efficiency decreases with increasing contact pressure. As mentioned earlier, friction is the result of two mechanisms: the formation of a lubricating ‘cushion’ separating the rubbing surfaces and the resistance associated with the mechanical interaction of the surface asperities of the tool and steel sheet. The higher the contact pressure, the greater the share of the latter mechanism. Under these conditions, the lubrication efficiency is at a much higher level (13.5–20.5% for $p_L = 12$ bar and 15.3–33% for $p_L = 18$ bar) compared with the tests carried out at a lubricant pressure of $p_L = 6$ bar.

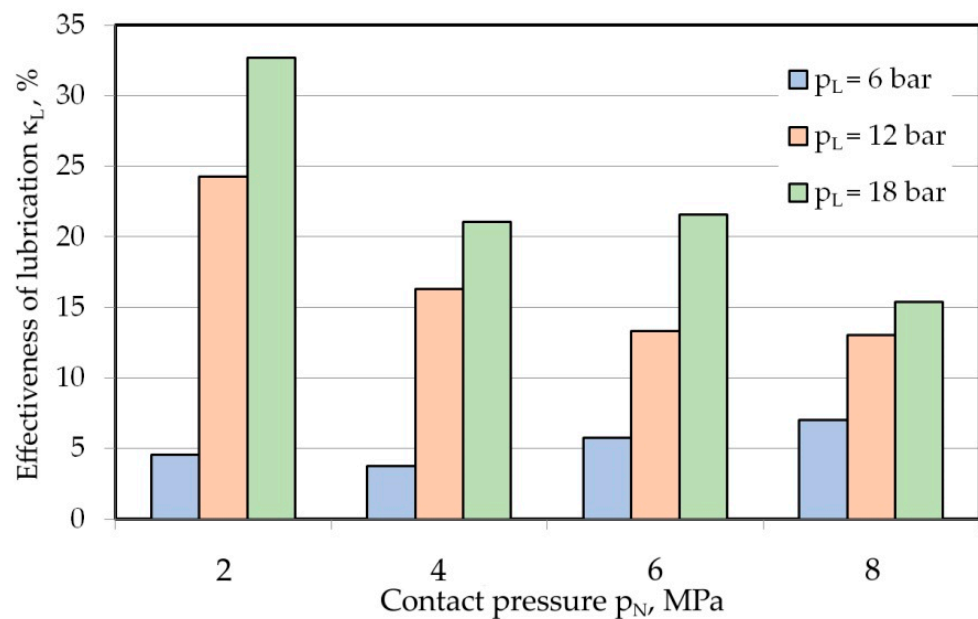


Figure 9. Effectiveness of lubrication ε_L for lubrication with S100 Plus oil.

For the range of applied contact pressures between 2 and 6 MPa, the efficiency of lubrication with S300 oil at $p_L = 6$ bar (Figure 10) was higher than for S100 Plus oil (Figure 9). Comparing the lubrication efficiency for the other lubricant pressures does not give such an unambiguous answer. Similarly, as the contact pressure increases, lubrication efficiency decreases. At a lubricant pressure of $p_L = 12$ bar, the lubrication efficiency is much more even over the entire range of tested pressures compared with tests with S100 Plus oil. Very similar values of lubrication efficiency were obtained during the tests with these two oils. It can, therefore, be concluded that, at the highest lubricant pressure ($p_L = 18$ bar) and contact pressures of $p_N = 4$ –8 MPa, the viscosity of the lubricant does not significantly affect the lubrication efficiency. Only at the smallest contact pressure of $p_N = 2$ MPa did the lubricant with higher viscosity (S300) provide about 8% greater lubrication efficiency compared with the S100 oil with lower viscosity.

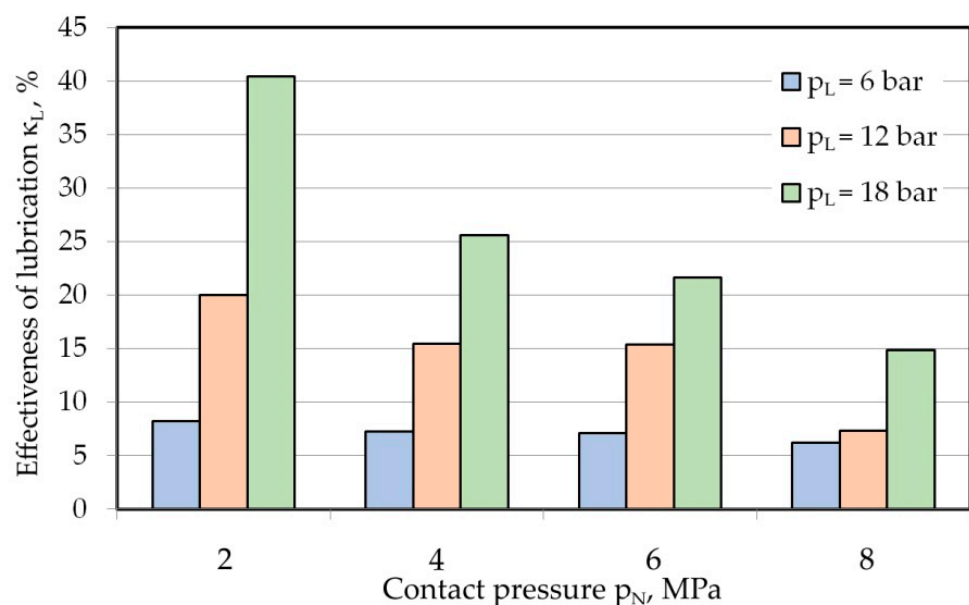


Figure 10. Effectiveness of lubrication ε_L for lubrication with S300 oil.

3.3. Surface Roughness

After the friction process, a decrease in the root mean square roughness parameter R_q for both tested oils was observed (Figure 11). In the absence of lubricant pressure and in the conditions of friction tests under a contact pressure of $p_N = 2$ MPa, reduction in roughness was greater when lubricated with S100 Plus oil compared with S300 oil. In general, due to the synergistic effect of lubricant pressure and contact pressure on the changes in surface topography, the roughness of the as-received sheet metal ($S_q = 1.82 \mu\text{m}$) decreased to about 1.3–1.68 μm .

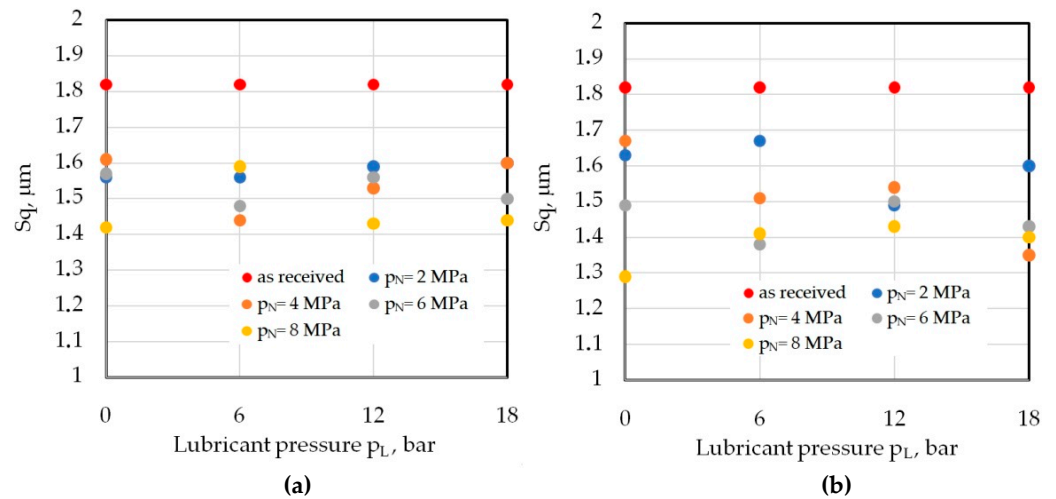


Figure 11. Effect of lubricant pressure on the S_q parameter for lubrication with (a) S100 Plus oil and (b) S300 oil.

The kurtosis S_{ku} similarly to the S_q parameter also decreased for the specimens subjected to friction (Figure 12). The kurtosis of the as-received surface shows deep valleys or unexpectedly high peaks ($S_{ku} > 3$) on the surface. The summits of the sheet asperities after friction were sheared or deformed; therefore, $S_{ku} < 3$. Surface wear due to friction reduces the S_{ku} value. In SMF processes, the surface of the tool is made of a material with much greater mechanical strength than the sheet material, which undergoes intentional plastic deformations. In the process of friction, the kurtosis of the surface S_{ku} is one of the most important parameters indicating a change in the height of the surface profile [50].

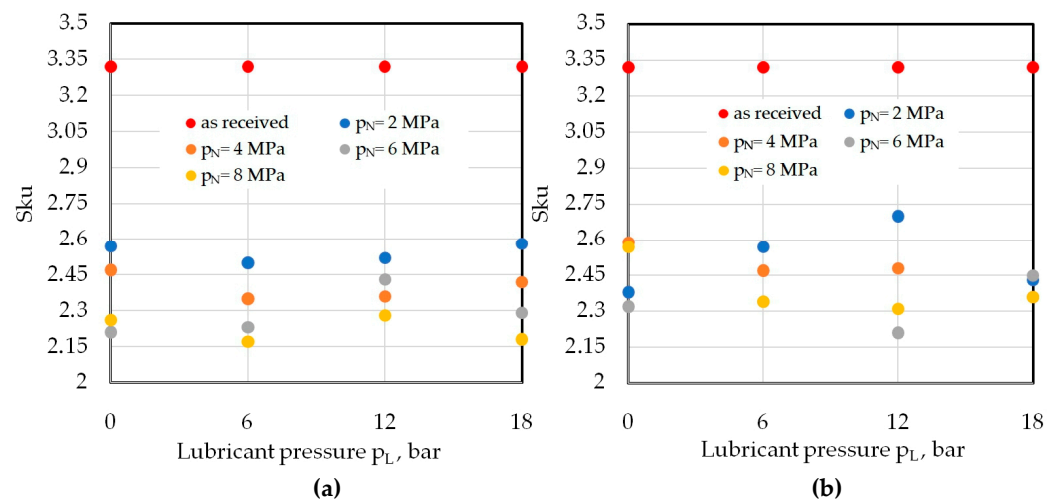


Figure 12. Effect of lubricant pressure on surface kurtosis S_{ku} for lubrication with (a) S100 Plus oil and (b) S300 oil.

The skewness S_{sk} provides information about the surface asymmetry. The valley-dominant surface is characterized by $S_{sk} < 0$, while the peak-dominant surface is characterized by $S_{sk} > 0$ [17]. In addition to the S_q parameter, the S_{sk} and S_{ku} parameters describe the surface roughness of sheets in industrial practice [34,51]. Moreover, an increase in kurtosis and skewness leads to an increase in the contact area ratio (the ratio between the real contact area and nominal contact area) of the sheet surface [52]. During friction for the highest pressure value, the skewness S_{sk} values are negative or close to 0 (Figure 13), which means the surface is characterized by a high load capacity resulting from the lack of high summits. A local increase in the skewness value at the highest values of lubricant and contact pressure means the activation of the flattening mechanism [53,54]. Under these conditions, the phenomenon of intensive flattening and plowing occurs, causing the formation of grooves (Figure 14) of various depths on the surface of the sheet. Figure 15 shows the surface profiles of the DC01 steel sheet before and after friction tests.

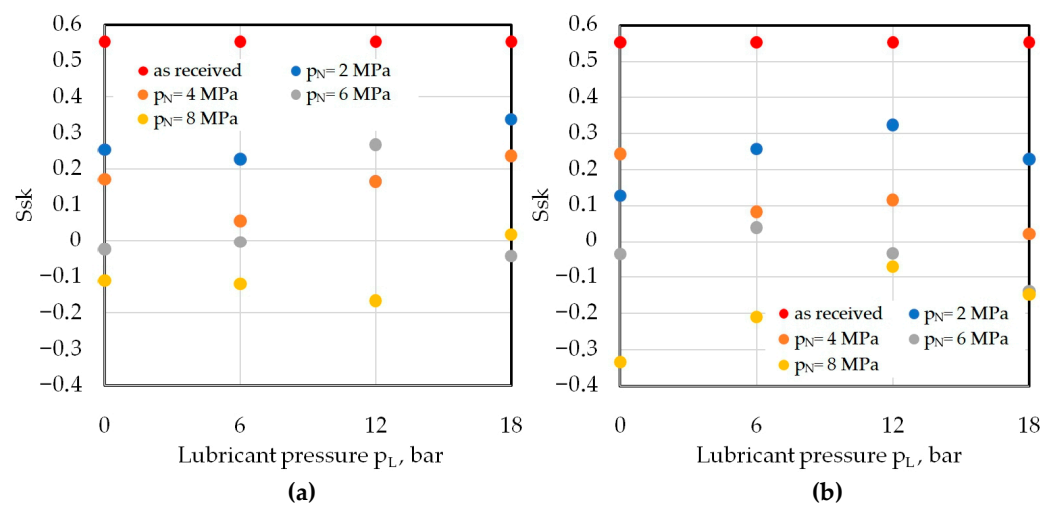


Figure 13. Effect of lubricant pressure on the surface skewness S_{sk} for lubrication with (a) S100 Plus oil and (b) S300 oil.

Figure 16 presents the effect of friction conditions on the changes in the parameters S_q , S_{sk} , S_{ku} , and S_z in conditions without forced lubricant pressure ($p_L = 0$ bar). Changing the friction conditions by using S300 oil instead of S100 Plus oil with almost three times lower viscosity reduces the S_q (Figure 16a) and S_{sk} (Figure 16b) parameters for the applied contact pressures of $p_N = 6$ – 8 MPa. At contact pressures of $p_N = 2$ – 4 MPa, the change in the above-mentioned parameters is insignificant in the range of 1.56 – 1.67 μm and 0.13 – 0.25 for the S_q and S_{sk} parameters, respectively. For the contact pressure of $p_N = 6$ MPa, the real contact area of the surface profile was stabilized, and the change in the type of the lubricant did not change the value of the S_{sk} parameter (Figure 16b). An increase in the value of the S_q parameter under the contact pressure of 2 – 4 MPa in relation to the dry friction conditions (Figure 16a) is due to lubricant entrapment. For the same lubrication conditions, but with a contact pressure of $p_N = 8$ MPa, lubrication reduces the S_q parameter compared with dry friction. The lubricant pressure was sufficient to limit the mechanical interaction of the surface asperities, while high values of contact pressures increased the real contact area.

Kurtosis is a measure of the flattening of the surface compared with the normal distribution—it is the basic identifier of the shape of the probability distribution. For a Gaussian distribution, the S_{ku} kurtosis value is 3.0 . The value of the kurtosis of the original sheet surface ($S_{ku} = 3.32$, Figure 16c) indicates a more convex distribution than a Gaussian distribution. However, after the friction process, all the tested sheets showed a distribution flatter than a Gaussian distribution ($S_{ku} < 2.6$). Increasing the value of the contact pressure from 2 MPa to 4 MPa resulted in the reduction of the S_z parameter in

all analyzed friction conditions (Figure 16d). This parameter is an appropriate indicator to determine the moment when lubricating film breaks and the sheet metal surface is plowed by the surface asperities of the tool's surface. For the conditions of lubrication with S100 Plus oil, a similar character of changes in the S_z parameter was observed. At contact pressures of 4 and 6 MPa, S300 oil provided a thicker lubricant due to its higher viscosity compared with S100 Plus oil. In this way, under these conditions, a lower value of the S_z parameter was observed. When the contact pressure was further increased to $p_N = 8$ MPa, unfortunately, the S300 oil lost its ability to effectively separate rubbing surfaces; hence, the value of the S_z parameter was at a similar level as during the tests for the dry friction conditions.

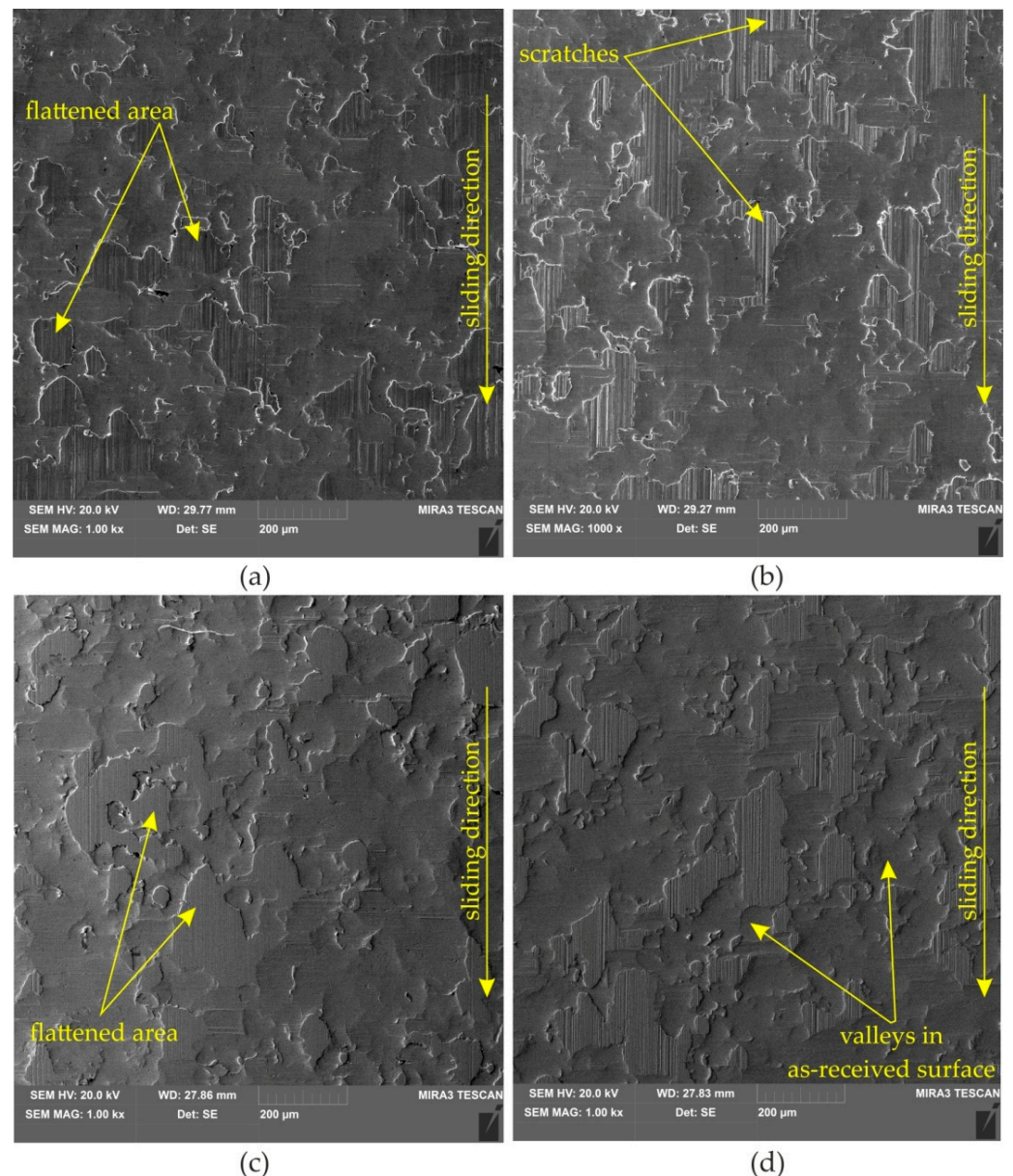


Figure 14. SEM micrographs of specimen surfaces tested under the following conditions: (a) S100 Plus oil, $p_N = 4$ MPa, $p_L = 0$ bar; (b) S100 Plus oil, $p_N = 4$ MPa, $p_L = 6$ bar; (c) S100 Plus oil, $p_N = 4$ MPa, $p_L = 12$ bar; (d) S100 Plus oil, $p_N = 4$ MPa, $p_L = 18$ bar.

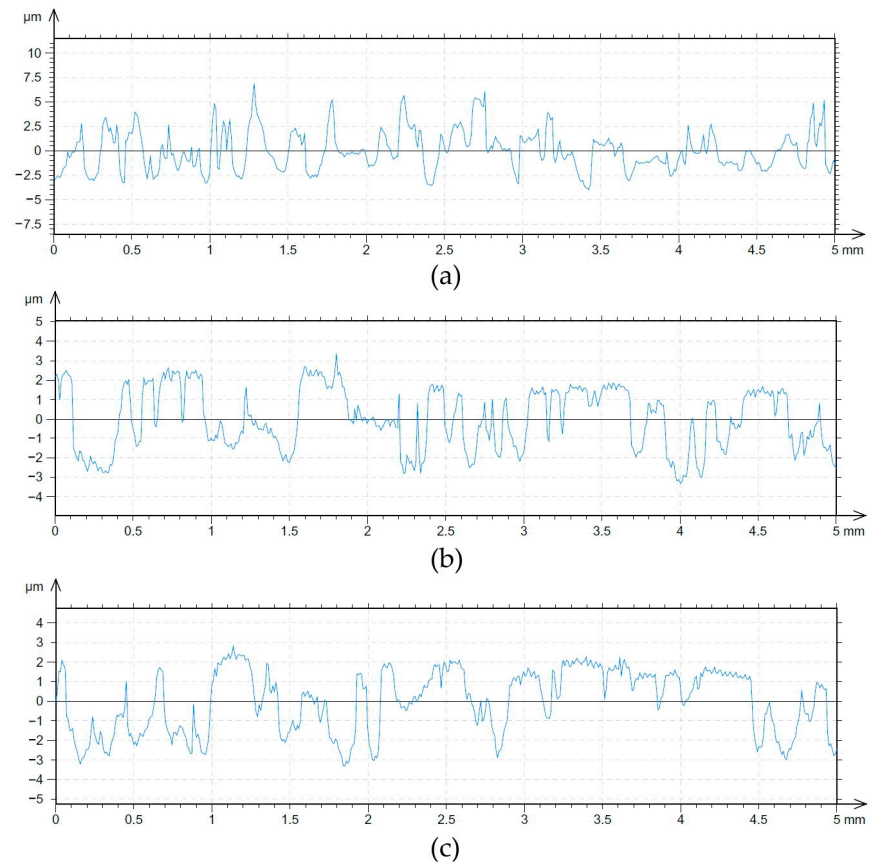


Figure 15. Surface profile of DC01 steel sheet in (a) as-received state and after friction tests carried out under the following conditions: (b) $p_L = 8$ bar, $p_N = 12$ MPa, S100 Plus oil; (c) $p_L = 8$ bar, $p_N = 12$ MPa, S300 oil.

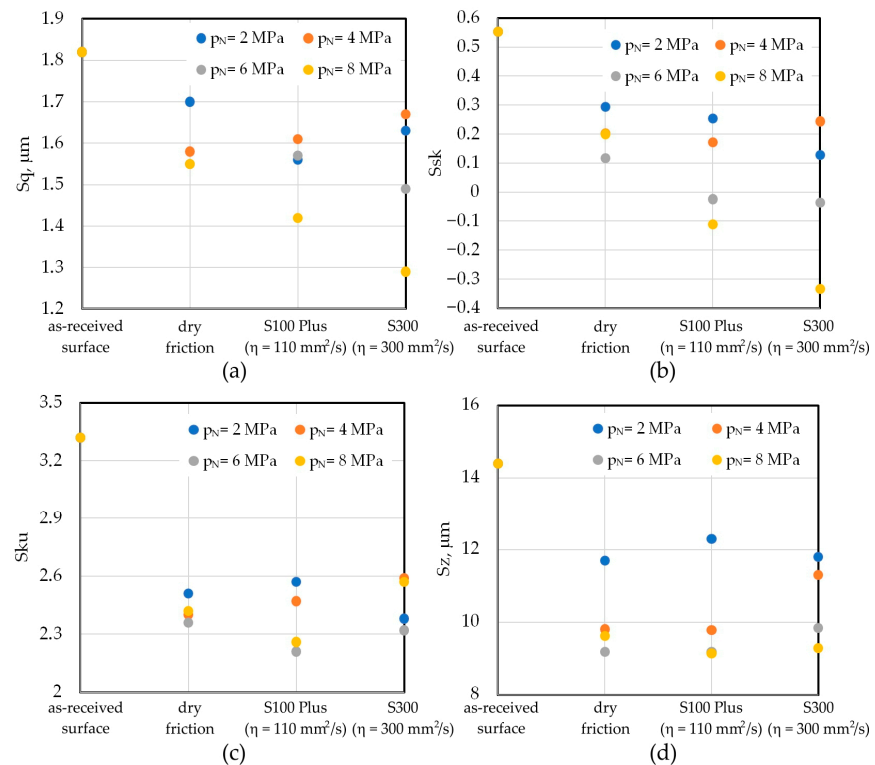


Figure 16. Effect of friction conditions on (a) S_q , (b) S_{sk} , (c) S_{ku} , and (d) S_z .

4. Conclusions

In this paper, an approach to reducing the COF in SMF by directly applying pressurized oil to the contact zone was investigated. Strip drawing tests were performed for contact pressures commonly occurring in the blankholder zone in SMF. Experimental studies carried out using the SDT are the basis for drawing the following conclusions:

- The COF decreases with increasing lubricant pressure for contact pressures p_N of 2–6 MPa. For the contact pressure of 8 MPa, the lubricant pressure has the least favorable effect of reducing the COF.
- Increasing the oil pressure has a positive effect on the reduction of friction, but its value is limited by the possible occurrence of leaks from the contact zone. Therefore, the lubricant pressure must be properly selected for the size of the nominal contact surface.
- Conventional lubrication ($p_L = 0$ MPa) without the forced supply of oil under pressure causes only a slight increase in the COF with increasing contact pressures. This fact was observed for both oils tested.
- The value of the COF is the resultant of the effect of the lubricating film. The use of oil with a higher viscosity allows the development of the mechanical interaction of the surface asperities to be delayed.
- At the lowest applied lubricant pressures ($p_L = 6$ bar), the lubrication efficiency was similar over the nominal pressures $p_N = 2$ –8 MPa.
- At the higher lubricant pressures $p_L = 12$ bar and $p_L = 18$ bar, the lubrication efficiency depends on the viscosity of the oil and decreases with increasing nominal pressure.
- The values of the analyzed roughness parameters S_p , S_{sk} , and S_{ku} decreased. There is a tendency for the S_{ku} parameter to decrease with increasing lubricant pressure.

Author Contributions: Conceptualization, T.T., K.S. and M.S.; methodology, T.T., K.S. and M.S.; validation, T.T., K.S. and M.S.; investigation, T.T., K.S. and M.S.; data curation, T.T., K.S. and M.S.; writing—original draft preparation, K.S. and T.T.; writing—review and editing, T.T. All authors have read and agreed to the published version of the manuscript.

Funding: This research received no external funding.

Institutional Review Board Statement: Not applicable.

Informed Consent Statement: Not applicable.

Data Availability Statement: Data is contained within the article.

Conflicts of Interest: The authors declare no conflict of interest.

References

1. Gronostajski, Z.; Pater, Z.; Madej, L.; Gontarz, A.; Lisiecki, L.; Łukaszek-Sołek, A.; Łuksza, J.; Mróz, S.; Muskalski, Z.; Muzykiewicz, W. Recent development trends in metal forming. *Arch. Civ. Mech. Eng.* **2019**, *19*, 898–941. [[CrossRef](#)]
2. Sigvant, M.; Pilthammar, J.; Hol, J.; Wiebenga, J.H.; Chezan, T.; Carleer, B.; van den Boogaard, T. Friction in sheet metal forming: Influence of surface roughness and strain rate on sheet metal forming simulation results. *Procedia Manuf.* **2019**, *29*, 512–519. [[CrossRef](#)]
3. Schmoeckel, D.; Frontzek, H.; von Finckenstein, E. Reduction of Wear on Sheet Metal Forming Tools. *CIRP Ann.* **1986**, *35*, 195–198. [[CrossRef](#)]
4. Bang, J.; Song, J.; Bae, G.; Park, N.; Lee, M.; Kim, H. Quantitative evaluation of experimental wear behaviour for CrN-coated tool steels in sheet metal forming process of TRIP 1180. *Procedia Manuf.* **2020**, *50*, 791–794. [[CrossRef](#)]
5. Domitner, J.; Silvayeh, Z.; Sabet, A.S.; Öksüz, K.I.; Pelcastre, L.; Hardell, J. Characterization of wear and friction between tool steel and aluminum alloys in sheet forming at room temperature. *J. Manuf. Process.* **2021**, *64*, 774–784. [[CrossRef](#)]
6. Trzepieciński, T.; Lemu, H.G. Study on frictional conditions of AA5251 aluminium alloy sheets using drawbead simulator test and numerical methods. *Stroj. Vestn. J. Mech. Eng.* **2014**, *60*, 51–60. [[CrossRef](#)]
7. Wang, D.; Yang, H.; Li, H. Advance and trend of friction study in plastic forming. *Trans. Nonferr. Met. Soc. China* **2014**, *24*, 1263–1272. [[CrossRef](#)]
8. Nie, N.; Su, L.; Deng, G.; Li, H.; Yu, H.; Tieu, A.K. A review on plastic deformation induced surface/interface roughening of sheet metallic materials. *J. Mater. Res. Technol.* **2021**, *15*, 6574–6607. [[CrossRef](#)]

9. Assemien, M.; Le Bot, A. Influence of sliding speed on roughness noise. In Proceedings of the 26th International Congress on Sound and Vibration, Montreal, QC, Canada, 7–11 July 2019; pp. 1–6.
10. Wu, Y.; Recklin, V.; Groche, P. Strain Induced Surface Change in Sheet Metal Forming: Numerical Prediction, Influence on Friction and Tool Wear. *J. Manuf. Mater. Process.* **2021**, *5*, 29. [[CrossRef](#)]
11. Juanjuan, H.; Jie, Z.; Wei, Z.; Guangchun, W. Influence of metal forming parameters on surface roughness and establishment of surface roughness prediction model. *Int. J. Mech. Sci.* **2019**, *163*, 105093.
12. Trzepieciński, T.; Gelgele, H.L. Investigation of anisotropy problems in sheet metal forming using finite element method. *Int. J. Mater. Form.* **2011**, *4*, 357–359. [[CrossRef](#)]
13. Trzepieciński, T. 3D elasto-plastic FEM analysis of the sheet drawing of anisotropic steel sheet metals. *Arch. Civ. Mech. Eng.* **2010**, *10*, 95–106. [[CrossRef](#)]
14. Yang, T.S. Prediction of surface topography in lubricated sheet metal forming. *Int. J. Mach. Tools Manuf.* **2008**, *48*, 768–777. [[CrossRef](#)]
15. Bello, D.O.; Walton, S. Surface topography and lubrication in sheet-metal forming. *Tribol. Int.* **1987**, *20*, 59–65. [[CrossRef](#)]
16. Evin, E.; Tomáš, M.; Výrostek, M. Verification the numerical simulation of the strip drawing test by its physical model. *Acta Mech. Slovaca* **2016**, *20*, 14–21. [[CrossRef](#)]
17. Trzepieciński, T.; Fejkiel, R. On the influence of deformation of deep drawing quality steel sheet on surface topography and friction. *Tribol. Int.* **2017**, *115*, 78–88. [[CrossRef](#)]
18. Masters, L.G.; Williams, D.K.; Roy, R. Friction behaviour in strip draw test of pre-stretched high strength automotive aluminium alloys. *Int. J. Mach. Tools Manuf.* **2013**, *73*, 17–24. [[CrossRef](#)]
19. Więckowski, W.; Adamus, J.; Dwyer, M.; Motyka, M. Tribological Aspects of Sheet Titanium Forming. *Materials* **2023**, *16*, 2224. [[CrossRef](#)]
20. Lovell, M.R.; Deng, Z. Characterization of interfacial friction in coated sheet steels: Influence of stamping process parameters and wear mechanisms. *Tribol. Int.* **2002**, *35*, 85–95. [[CrossRef](#)]
21. Gierzyńska, M. *Tarcie, Zużycie i Smarowanie w Obróbce Plastycznej Metali*; Wydawnictwa Naukowo-Techniczne: Warszawa, Poland, 1983.
22. Wang, G.; Guo, B.; Shan, D. Friction related size-effect in microforming—A review. *Manuf. Rev.* **2014**, *1*, 23. [[CrossRef](#)]
23. Lowell, M.; Higgs, C.F.; Deshmukh, P.; Mobley, A. Increasing formability in sheet metal stamping operations using environmentally friendly lubricants. *J. Mater. Process. Technol.* **2006**, *177*, 87–90.
24. Więckowski, W.; Adamus, J.; Dwyer, M. Sheet metal forming using environmentally benign lubricant. *Arch. Civ. Mech. Eng.* **2020**, *20*, 51. [[CrossRef](#)]
25. Lachmayer, R.; Behrens, B.-A.; Ehlers, T.; Müller, P.; Althaus, P.; Oel, M.; Farahmand, E.; Gembarski, P.C.; Wester, H.; Hübner, S. Process-Integrated Lubrication in Sheet Metal Forming. *J. Manuf. Mater. Process.* **2022**, *6*, 121. [[CrossRef](#)]
26. Kawasegi, N.; Sugimori, H.; Morimoto, H.; Morita, N.; Hori, I. Development of cutting tools with microscale and nanoscale textures to improve frictional behaviour. *Precis. Eng.* **2009**, *33*, 248–254. [[CrossRef](#)]
27. Geiger, M.; Roth, S.; Becker, W. Influence of laser-produced microstructures on the tribological behavior of ceramics. *Surf. Coat. Technol.* **1998**, *100–101*, 17–22. [[CrossRef](#)]
28. Kim, D.E.; Cha, K.H.; Sung, I.H.; Bryan, J. Design of surface micro-structures for friction control in micro-systems applications. *CIRP Ann. Manuf. Technol.* **2002**, *51*, 495–498. [[CrossRef](#)]
29. Costa, H.L.; Hutchings, I.M. Hydrodynamic lubrication of textured steel surfaces under reciprocating sliding conditions. *Tribol. Int.* **2007**, *40*, 1227–1238. [[CrossRef](#)]
30. Kummel, J.; Braun, D.; Gibmeier, J.; Schneider, J.; Greiner, C.; Schulze, V.; Wanner, A. Study on micro texturing of uncoated cemented carbide cutting tools for wear improvement and built-up edge stabilisation. *J. Mater. Process. Technol.* **2015**, *215*, 62–70. [[CrossRef](#)]
31. Wang, L. Use of structured surfaces for friction and wear control on bearing surfaces. *Surf. Topogr. Metrol. Prop.* **2014**, *2*, 43001. [[CrossRef](#)]
32. Abdel Aal, H.A. Functional surfaces for tribological applications: Inspiration and design. *Surf. Topogr. Metrol. Prop.* **2016**, *4*, 43001. [[CrossRef](#)]
33. Mousavi, A.; Sperk, T.; Gietzelt, T.; Kunze, T.; Lasagni, A.F.; Brosius, A. Effect of contact area on friction force in sheet metal forming operations. *Key Eng. Mater.* **2018**, *767*, 77–84. [[CrossRef](#)]
34. Sedlaček, M.; Podgornik, B.; Vižintin, J. Influence of surface preparation on roughness parameters, friction and wear. *Wear* **2009**, *266*, 482–487. [[CrossRef](#)]
35. Xie, H.C.; Chen, D.R.; Kong, X.M. An analysis of the three-dimensional surface topography of textured cold-rolled steel sheets. *Tribol. Int.* **1999**, *32*, 83–87. [[CrossRef](#)]
36. Zavadil, J.; Bartunek, J.S.; Fojtik, D. Analysis of periodicities in surface topography of cold rolled sheets using data captured by camera system. *Meas. Sci. Rev.* **2020**, *20*, 145–149. [[CrossRef](#)]
37. Bay, N.; Olsson, D.D.; Andreasen, J.L. Lubricant test methods for sheet metal forming. *Tribol. Int.* **2018**, *41*, 844–853. [[CrossRef](#)]
38. Trzepieciński, T.; Lemu, H.G. Recent developments and trends in the friction testing for conventional sheet metal forming and incremental sheet forming. *Metals* **2020**, *10*, 47. [[CrossRef](#)]
39. Erbel, S.; Kuczyński, K.; Marciniak, Z. *Cold Plastic Working*; PWN: Warsaw, Poland, 1975.

40. Prakash, V.; Kumar, D.R. Performance evaluation of bio-lubricants in strip drawing and deep drawing of an aluminium alloy. *Adv. Mater. Process. Technol.* **2022**, *8*, 1044–1057. [[CrossRef](#)]
41. ISO 25178–2:2022; Geometrical Product Specifications (GPS)—Surface Texture: Areal—Part 2: Terms, Definitions and Surface Texture Parameters. International Organization for Standardization: Geneva, Switzerland, 2022.
42. Cillaurren, J.; Galdos, L.; Sanchez, M.; Zabala, A.; Saenz de Argandoña, E.; Mendiguren, J. Contact pressure and sliding velocity ranges in sheet metal forming simulations. In Proceedings of the 24th International Conference on Material Forming ESAFORM 2021, Liège, Belgium, 14–16 April 2021.
43. Djordjević, M.; Aleksandrović, S.; Djačić, S.; Sedmak, A.; Lazić, V.; Arsić, D.; Mutavdžić, M. Simulation of flat die deep drawing process by variable contact pressure sliding model. *Teh. Vjesn.* **2019**, *26*, 1199–1204.
44. Filzek, J.; Groche, P. *Assessment of the Tribological Function of Lubricants for Sheet Metal Forming. Bench Testing of Industrial Fluid Lubrication and Wear Properties Used in Machinery Applications*, ASTM STP 1404; Totten, G.E., Wedeven, L.D., Dickey, J.R., Anderson, M., Eds.; American Society for Testing and Materials: West Conshohocken, PA, USA, 2001.
45. Steiner, J.; Andreas, K.; Merklein, M. Investigation of surface finishing of carbon based coated tools for dry deep drawing of aluminium alloys. *IOP Conf. Ser. Mater. Sci. Eng.* **2016**, *159*, 012022. [[CrossRef](#)]
46. Jewvattanarak, P.; Mahayotsanun, N.; Mahabunphachai, S.; Ngernbamrung, S.; Dohda, K. Tribological effects of chlorine-free lubricant in strip drawing of advanced high strength steel. *Proc. Inst. Mech. Eng. Part J J. Eng. Tribol.* **2016**, *230*, 974–982. [[CrossRef](#)]
47. De Andragoña, E.S.; Zabala, A.; Galdos, L.; Mendiguren, J. The Effect of Material Surface Roughness in Aluminum Forming. *Procedia Manuf.* **2020**, *47*, 591–595. [[CrossRef](#)]
48. Abe, Y.; Mori, K.; Hatashita, F.; Shiba, T.; Daodon, W.; Osakada, K. Improvement of seizure resistance in ironing of stainless steel cup with cermet die having fine lubricant pockets. *J. Mater. Process. Technol.* **2016**, *234*, 195–207. [[CrossRef](#)]
49. George, E.; Kurien, G.E.; Vishal, U.; Anil, P.M. A Study on The Effect of Oil Pocket Density on The Effectiveness of Boundary Lubrication in the Liner-ring Interface. *Procedia Eng.* **2013**, *64*, 1062–1068. [[CrossRef](#)]
50. Pereira, T.G.; Hernández, A.; Martínez, P.; Pérez, J.; Mathia, J.A. Surface topographic characterization for polyamide composite injection molds made of aluminum and copper alloy. *Scanning* **2014**, *36*, 39–52. [[CrossRef](#)]
51. Sedlaček, M.; Vilhena, L.M.S.; Podgornik, B.; Vižintin, J. Surface topography modelling for reduced friction. *Stroj. Vestn. J. Mech. Eng.* **2011**, *57*, 674–680. [[CrossRef](#)]
52. Wang, W.Z.; Chen, H.; Hu, Y.Z.; Wang, H. Effect of surface roughness parameters on mixed lubrication characteristics. *Tribol. Int.* **2006**, *39*, 522–527. [[CrossRef](#)]
53. Žaba, K.; Kuczek, Ł.; Puchlerska, S.; Wiewióra, M.; Góral, M.; Trzepieciński, T. Analysis of Tribological Performance of New Stamping Die Composite Inserts Using Strip Drawing Test. *Adv. Mech. Mater. Eng.* **2023**, *40*, 55–62. [[CrossRef](#)]
54. Szewczyk, M.; Sz wajka, K. Assessment of the Tribological Performance of Bio-Based Lubricants Using Analysis of Variance. *Adv. Mech. Mater. Eng.* **2023**, *40*, 31–38. [[CrossRef](#)]

Disclaimer/Publisher’s Note: The statements, opinions and data contained in all publications are solely those of the individual author(s) and contributor(s) and not of MDPI and/or the editor(s). MDPI and/or the editor(s) disclaim responsibility for any injury to people or property resulting from any ideas, methods, instructions or products referred to in the content.